Gap junctional hemichannel-mediated ATP release and hearing controls in the inner ear

Hong-Bo Zhao*, Ning Yu, and Carrie R. Fleming

Department of Surgery–Otolaryngology, University of Kentucky Medical Center, Lexington, KY 40536-0293

Edited by Michael V. L. Bennett, Albert Einstein College of Medicine, Bronx, NY, and approved October 21, 2005 (received for review July 28, 2005)

Connexin gap junctions play an important role in hearing function, but the mechanism by which this contribution occurs is unknown. Connexins in the cochlea are expressed only in supporting cells; no connexin expression occurs in auditory sensory hair cells. A gap junctional channel is formed by two hemichannels. Here, we show that connexin hemichannels in the cochlea can release ATP at levels that account for the submicromolar concentrations measured in the cochlear fluids *in vivo*. The release could be increased 3- to 5-fold by a reduction of extracellular Ca^{2+} or an increase in membrane stress, and blocked by gap junctional blockers. We also demonstrated that extracellular ATP at submicromolar levels apparently affected outer hair cell (OHC) electromotility, which is an active cochlear amplifier determining cochlear sensitivity to sound stimulation in mammals. ATP reduced OHC electromotility and the slope factor of the voltage dependence and shifted the operating point to reduce the active amplifier gain. ATP also reduced the generation of distortion products. Immunofluorescent staining showed that purinergic receptors P2x2 and P2x7 were distributed on the OHC surface. Blockage of P2 receptors eliminated the effect of ATP on the OHC electromotility. The data revealed that there is a hemichannel-mediated, purinergic intercellular signaling pathway between supporting cells and hair cells in the cochlea to control hearing sensitivity. The data also demonstrated a potential source of ATP in the cochlea.

active cochlear mechanics | cochlear supporting cells | connexin | outer hair cell electromotility | P2 receptor

Connexin gap junctions are important for hearing function. Connexin mutations are associated with a high incidence of hearing loss; they are responsible for 70–80% of nonsyndromic hearing loss in children (1). The pathogenesis mainly occurs in the inner ear. In the mammalian cochlea, connexins are expressed extensively in nonsensory supporting cells, but no connexin expression is observed in auditory sensory hair cells (2, 3). Hypothetical functions of gap junctional coupling in the cochlea include nutrition, K^+-recycling, and metabolic communication (4–6). However, how connexin function influences auditory hearing remains unclear.

Gap junctions are cytoplasmic conduits possessing large pore size (10–15 Å) and allowing the passage of small metabolites and signaling molecules (<1–1.2 kDa) between cells. Each gap junctional channel is composed of two hemichannels; each hemichannel is composed of six connexin subunits (7, 8). Newly assembled hemichannels randomly insert into the nonjunctional cell membrane and drift laterally to the gap junctional plaques. The hemichannel then docks with another hemichannel on the adjacent cell membrane to form a complete gap junctional channel between the two cells. Initially, it was thought that hemichannels would not open before formation of integral gap junction channels because of the possible lethal effect induced by their large conductance and pore size. However, recent experiments have documented that hemichannels can open on the nonjunctional cell surface by depolarization/hyperpolarization, membrane tension, reduction of extracellular Ca^{2+}, and metabolic stresses (9, 10). In this experiment, we document that hemichannels in the cochlear-supporting cells can function to release ATP under physiological conditions, and that this can affect outer hair cell (OHC) electromotility and hearing function. The data provide insight into connexin channels in supporting cells participating in regulation of hearing function, and also demonstrate an intercellular pathway between supporting cells and hair cells to control hearing sensitivity.

Materials and Methods

Cochlea Isolation and Incubation for ATP Measurement. The temporal bone was freshly isolated from adult guinea pigs (200–450 g) (6, 11–12). The cochlea was microdissected in a sterile normal extracellular solution (ECS) (142 mM NaCl/5.37 mM KCl/1.47 mM $MgCl_2$/2 mM $CaCl_2$/10 mM Hepes/25 mM dextrose/osmolarity 300 mOsm, pH 7.2) and was opened from its apex to base. After removal of the bone, stria vascularis, Reissner's membrane, and tectorial membrane, the organ of Corti was completely exposed. Then, the exposed cochlea was dissected from the temporal bone (Fig. 1*a*) and put into an incubation chamber. For testing hemichannel release, the isolated cochlea was incubated in 200 μl of ECS for 10 min and then incubated in an equal volume of a sterile nominally Ca^{2+}- and Mg^{2+}-free ECS (142 mM NaCl/5.37 mM KCl/10 mM Hepes/25 mM dextrose/300 mOsm, pH 7.2) for 15 min. Finally, the cochlea was reincubated in the normal ECS for 20 min. In every 5 min, the whole incubation solution (200 μl) was collected and replaced with fresh solution. Prior to collection of the incubation solution, gentle pipetting was performed one to two times for mixture. When switching to a solution with a new Ca^{2+} concentration, the cochlea was washed with the new solution one to two times before incubation. The osmolarity of all solutions was measured by a microcomputer controlled osmometer (Model 3300, Advanced Instruments, Norwood, MA) and adjusted by dextrose. All experiments were performed at room temperature (23°C).

Mechanical Stimulation and Membrane Stress. Mechanical stimulation was achieved by gently pipetting the incubated cochlea with micro glass beads. To test mechanical stimulus-induced ATP release, we used the same 10–15–20 min protocol as the Ca^{2+} reduction experiments. Mechanical stimulation was performed by replacing the nominally Ca^{2+}- and Mg^{2+}-free solution challenge with a normal ECS solution containing 10 mg/ml micro glass beads (ϕ = 30–50 μm, Polysciences). The solution containing the glass beads was gently pipetted (once per 3–4 s) with a 20-μl pipette in the 15-min period. The effect of membrane stress on ATP release was also tested by replacing the Ca^{2+}- and Mg^{2+}-free ECS with a hypotonic ECS (275 mOsm), which was

Conflict of interest statement: No conflicts declared.

This paper was submitted directly (Track II) to the PNAS office.

Abbreviations: ECS, extracellular solution; CBX, carbenoxolone; PL, perilymph; EL, endolymph; OHC, outer hair cell; PPADS, pyridoxalphosphate-6-azophenyl-2′,4′-disulfonic acid.

*To whom correspondence should be addressed at: Department of Surgery–Otolaryngology, University of Kentucky Medical Center, 800 Rose Street, Lexington, KY 40536-0293. E-mail: hzhao2@uky.edu.

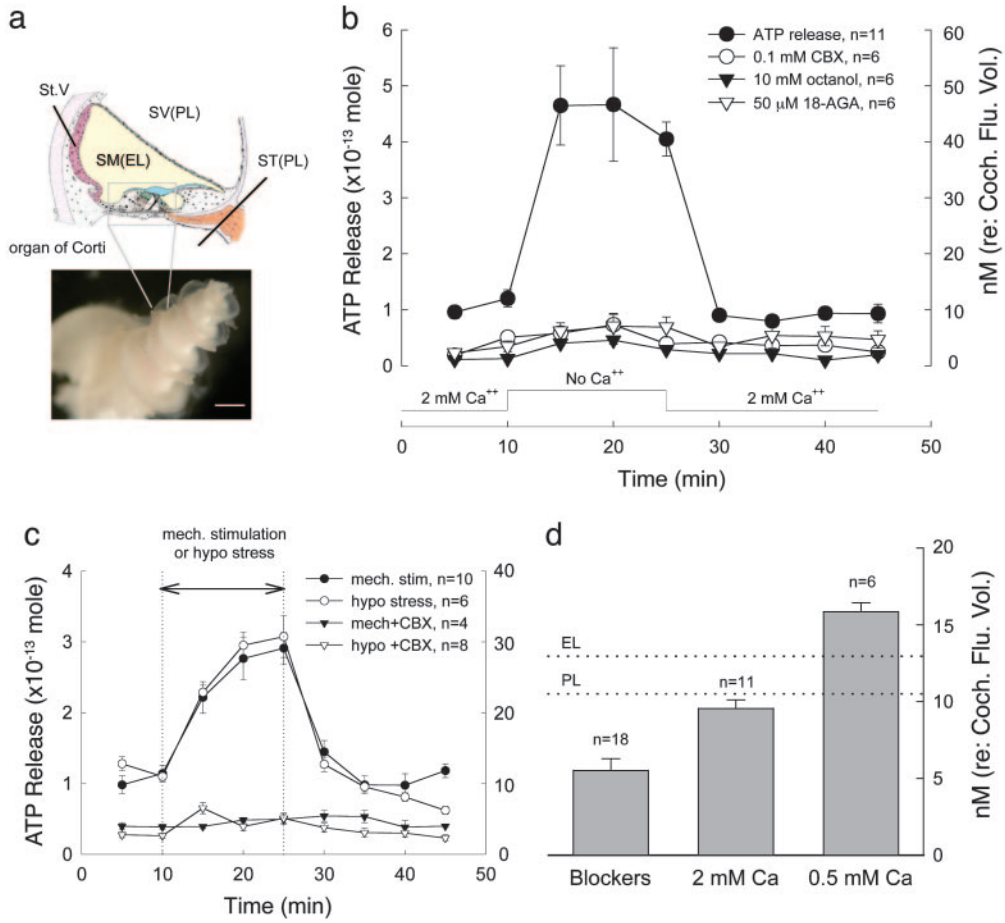

Fig. 1. ATP release from cochlear connexin hemichannels. (*a*) Diagram of the cross section of the cochlea and photograph of the dissected organ of Corti after removal of the embossed bone and stria vascularis (St. V) from the guinea pig inner ear. (Scale bar: 200 μm.) (*b*) ATP release after reduction of extracellular Ca^{2+}. Lines with different symbols represent the measured amounts of ATP released in controls and during treatment with gap junction blockers, 0.1 mM CBX, 10 mM octanol, and 50 μM 18α-glycyrrhetinic acid (18-AGA). The Ca^{2+} concentrations in the incubation solutions are indicated along the *x* axis. The right *y* axis indicates the concentration of ATP calculated for the total fluid space volume (10 μl) of the guinea pig cochlea. (*c*) Mechanical stimulation and membrane tension-induced ATP release. A pair of vertical lines indicates the period of mechanical stimulation with micro glass beads or challenge with a hypotonic ECS (275 mOsm). The amounts of ATP release are shown for these treatments with or without 0.1 mM CBX. (*d*) Concentrations of ATP released at different extracellular Ca^{2+} concentrations and at 2 mM Ca^{2+} with gap junction blockers. The dotted lines indicate the reported ATP concentrations in the EL and PL *in vivo*. (Error bars represent SE.)

adjusted by dextrose, following the same protocol described above for the Ca^{2+} reduction experiments (see Fig. 1*c*).

ATP Measurement. The collected incubation solutions were kept on ice. The amount of ATP was measured by a bioluminescent-based method by using an EDTA-containing luciferin-luciferase assay kit (FL-ASC, Sigma) following the manufacturer's instructions. The bioluminescence was read by a luminometer (TopCount NXT, Packard) by using a black 96-well plate to avoid optical cross-talk. The amount of ATP was calculated from the ATP standard curve, which was simultaneously measured from serially 10-diluted ATP standards in each experiment. The standard curve also served as an internal control for machine measurement, which showed a good linearity ($r = 0.9997$; Fig. 5*a*, which is published as supporting information on the PNAS web site).

OHC Patch Clamp Recording and Nonlinear Capacitance Measurement. The detailed method for OHC isolation and patch clamp recording can be found in our previous reports (11–12). Briefly, OHCs were freshly isolated from the guinea pig's cochlea. The auditory sensory epithelia were then microdissected from the cochlea and dissociated with trypsin (1 mg/ml) for 5–10 min. The isolated OHC was voltage-clamped by an Axopatch 200B amplifier under the whole-cell configuration, and the electromotility-associated nonlinear cell membrane capacitance was measured by Jclamp (SciSoft, New Haven, CT) by using a two-sinusoidal method. The stimulus consisted of the sum of two voltage sine waves (390.625 and 781.25 Hz, $V_{p-p} = 10$ mV), which was superimposed on a voltage ramp (−150 mV to +150 mV) to deliver to the patched cell (12). The capacitance was calculated by fast Fourier transform (FFT) analysis of AC responses (13). The nonlinear capacitance was fitted to the first derivative of a two-state Boltzmann function (11–13):

$$C_m = Q_{max}\frac{\frac{ze}{kT}\exp\left(\frac{-ze(V_m - V_{pk})}{kT}\right)}{\left(1+\exp\left(\frac{-ze(V_m - V_{pk})}{kT}\right)\right)^2} + C_{lin}, \quad [1]$$

where C_{lin} is the linear cell capacitance component, Q_{max} is the maximum charge transferred, V_{pk} is the potential that has an equal charge distribution corresponding to the peak of the capacitance curve, z is the number of elementary charge (e) determining the slope of the voltage dependence, k is Boltz-

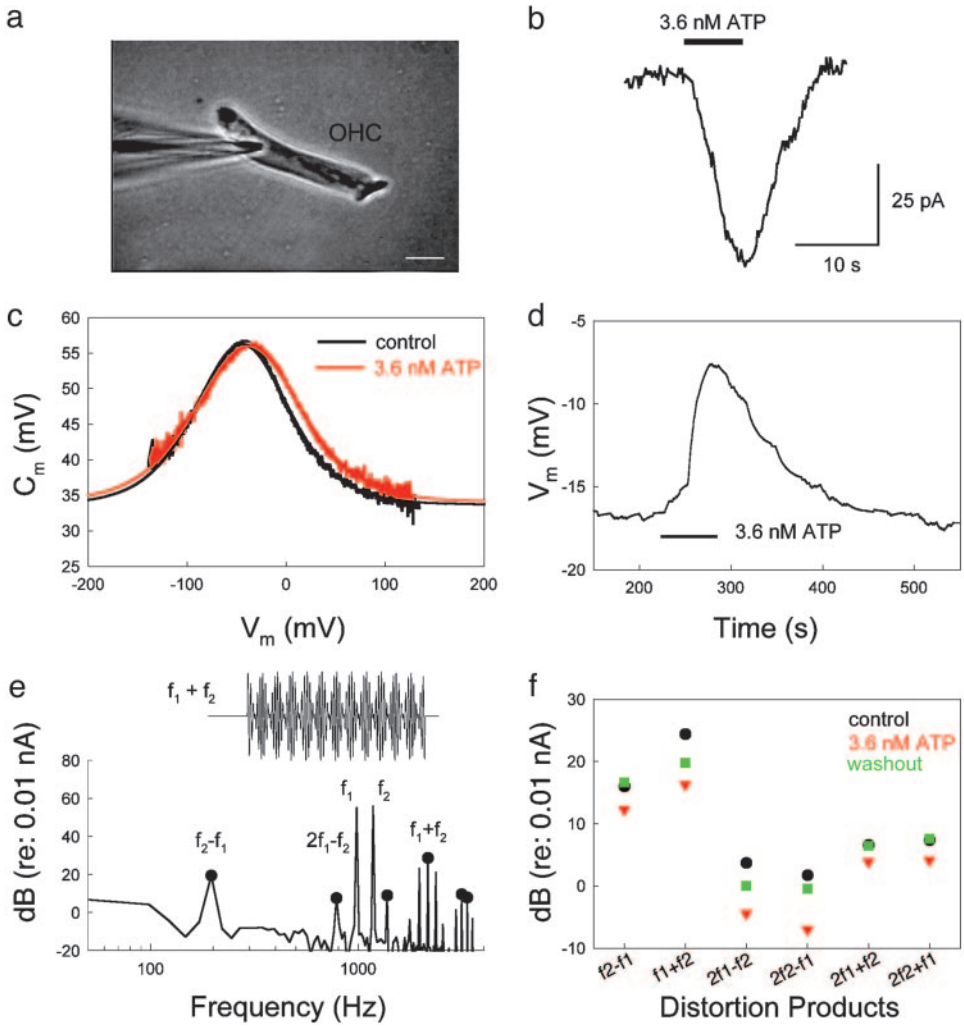

Fig. 2. Effects of ATP on OHC electromotility. (*a*) A captured image of patch clamp recording on an isolated OHC. (Scale bar: 10 μm.) (*b*) An ATP-induced inward current at $V_m = -40$ mV. (*c*) OHC electromotility-associated nonlinear capacitance. The black and red curves represent the nonlinear capacitance measured at control and perfusion of 3.6 nM ATP, respectively. The smooth bell-shape curves represent data fitting to the first derivative of the Boltzmann function. The parameters of fitting are $Q_{max} = 2.85$ and 3.13 pC, $z = 0.82$ and 0.72, $V_{pk} = -44.7$ and -38.2 mV, and $C_{lin} = 33.7$ and 34.1 pF for control and ATP perfusion, respectively. $R_s = 3.5$ MΩ. (*d*) ATP-induced reversible change in the peak voltage (V_{pk}) of nonlinear capacitance. The V_{pk} was continuously recorded by use of a phase-tracking technique (12, 13). A horizontal bar represents the extracellular perfusion of ATP. (*e*) The spectrum of OHC response to the two-sinusoidal voltage stimulation in patch clamp recording. The black solid circles indicate the components of quadric ($f_2 \pm f_1$) and cubic ($2f_1 \pm f_2$, $2f_2 \pm f_1$) distortions. (*Inset*) The voltage waveform of two added sinusoids, $f_1 = 977$ Hz and $f_2 = 1172$ Hz. (*f*) ATP-induced reduction in quadric and cubic distortion products. The black, red, and green symbols represent the distortion products at control, application of 3.6 nM ATP, and washout, respectively.

mann's constant, T is the absolute temperature, and V_m is the membrane potential that was corrected for electrode access resistance (R_s) and membrane resistance (R_m). Curve fitting and figure plotting were performed with SIGMAPLOT software. A Y-tube perfusion system was used for applications of ATP and chemicals in patch clamp recording.

Immunofluorescent Staining. Dissociated cochlear cells were fixed with 4% paraformaldehyde in 0.1 M PBS (pH 7.4) for 30 min. After washing with PBS, the cells were incubated in a blocking solution (10% goat serum and 1% BSA in the PBS) with 0.1% Triton X-100 for 20 min at room temperature. Then, the cells were incubated with anti-P2x2 or anti-P2x7 (P7892 and P8232, respectively, 1:200, Sigma) in the blocking solution at 4°C overnight. After washing with PBS, reaction to a 1:400 dilution of the secondary antibody conjugated with Alexa Fluor 488 (Molecular Probes) in the blocking solution was followed at room temperature for 1 h to visualize binding of the primary antibodies. Fluorescent images were photographed by a laser confocal microscope system.

Results

Connexin hemichannels can be opened to release ATP by reduction of extracellular Ca^{2+} concentration or mechanical stimulation. Fig. 1 shows that a reduction of extracellular Ca^{2+} or an increase in membrane tension induced ATP release. As the cochlea was incubated in the 0 mM Ca^{2+} ECS, the amount of ATP release increased from the $0.95 \pm 0.054 \times 10^{-13}$ mol baseline to $4.67 \pm 0.71 \times 10^{-13}$ mol (Fig. 1*b*). This release was an almost 5-fold reversible increase. When the cochlea was reincubated in the 2 mM Ca^{2+} ECS, the amount of ATP released had returned to the previous baseline. The gap junction blockers, carbenoxolone (CBX, 0.1 mM), octanol (10 mM), and 18α-glycyrrhetinic acid (18-AGA, 50 μM), which are known to block hemichannel dye uptake in cochlear-supporting cells (6), eliminated this increase. Interestingly, these gap junctional blockers

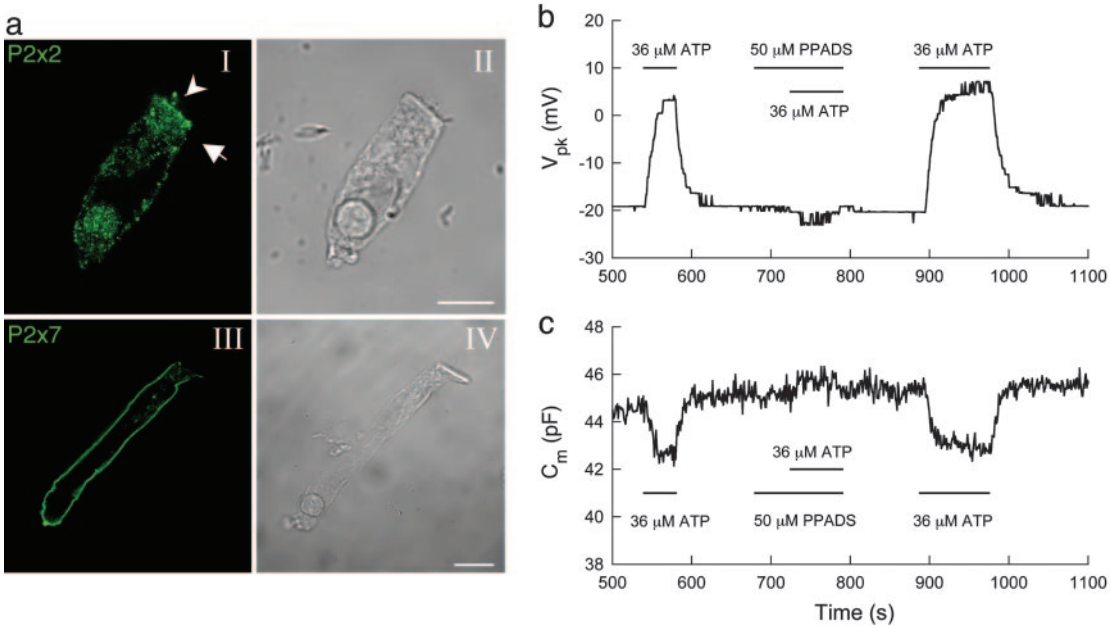

Fig. 3. ATP activates P2 receptors to affect OHC electromotility. (a) Immunofluorescent staining of OHCs for P2x2 and P2x7 purinergic receptors. An arrow head and arrow in *aI* indicate the stereocilia and cuticular plate, respectively, where strong fluorescent staining for P2x2 is visible. There is strong staining for P2x7 receptors on the basolateral wall (*aIII*). (Scale bars: 10 μm.) (*b* and *c*) Elimination of the effects of ATP on OHC electromotility by P2x receptor blocker PPADS. The V_{pk} (*b*) and nonlinear capacitance (*c*) were continuously recorded by use of a phase-tracking technique (12, 13). Horizontal bars represent the timing of chemical extracellular perfusion.

also significantly reduced the ATP release at 2 mM Ca^{2+} by 50% to $0.55 \pm 0.076 \times 10^{-13}$ mol ($n = 11$, Fig. 1*b*; $P < 0.001$, *t* test). Control experiments showed that these gap junctional blockers did not affect ATP measurement (Fig. 5). Blockage of either vesicular ATP release or ATP-binding cassette transporters also failed to inhibit this ATP release (Fig. 6, which is published as supporting information on the PNAS web site). Application of Bafilomycin A1 (3 μM) could reduce ATP release but still had a 2.7-fold increase in ATP release during no-Ca^{2+} ECS challenge (Fig. 6*b*).

The ATP release was Ca^{2+}-dependent. As extracellular Ca^{2+} increased, the release of ATP decreased. The average amounts of ATP released at 0.5 and 2 mM Ca^{2+} were 1.58 ± 0.059 ($n = 6$) and $0.95 \pm 0.054 \times 10^{-13}$ mol ($n = 11$), respectively. At 5 mM Ca^{2+}, the amount of ATP release was further reduced to $0.657 \pm 0.048 \times 10^{-13}$ mol ($n = 6$), which was not significantly different from the amount of ATP released at 2 mM Ca^{2+} with gap junctional blockers (Fig. 1*b*, $P > 0.1$, *t* test).

In Fig. 1 *b* and *c*, the right *y* axis indicates the concentration of the released ATP were it to occupy the volume of the cochlear fluid space. In the guinea pig cochlea, the volumes of the perilymph (PL) and endolymph (EL) are 8.65 and 1.2 μl, respectively, and the total volume of the cochlear fluid space is $\approx$10 μl (14). The amount of ATP released at 0 mM Ca^{2+} was $4.67 \pm 0.21 \times 10^{-13}$ mol ($n = 11$), and concentration referred to the total volume of the cochlear fluid space would be 46.6 ± 2.1 nM (Fig. 1*b*). At 0.5 and 2 mM Ca^{2+} levels, the concentrations of released ATP would be 15.8 ± 0.59 and 9.5 ± 0.54 nM, respectively (Fig. 1*d*). These concentrations were close to the reported ATP levels in the PL and EL, which are 10.5 ± 3.9 nM and 12.95 ± 2.4 nM, respectively (15), and are indicated by dotted lines in Fig. 1*d*.

Mechanical stimulation can also induce hemichannels to open and release ATP (16–20). Fig. 1*c* shows that the cochlear ATP release increased to $2.91 \pm 0.22 \times 10^{-13}$ mol during mechanical stimulation. After cessation of mechanical stimulation, the ATP level returned to the previous baseline (Fig. 1*c*). ATP release could also be elicited by increase in membrane tension. Application of a hypotonic ECS (275 mOsm) to raise cell membrane tension increased the ATP release to $3.07 \pm 0.29 \times 10^{-13}$ mol (Fig. 1*c*). CBX (0.1 mM) abolished both mechanical stimulation- and membrane tension-induced ATP release (Fig. 1*c*). Membrane stress-induced hemichannel ATP release is consistent with our previous report that connexin gap junctions in the cochlear-supporting cells are sensitive to membrane tension (21).

The organ of Corti contains auditory sensory inner hair cells and OHCs. The OHC has electromotility that can quickly change cell length to actively amplify basilar membrane vibrations and enhance auditory sensitivity (22–24). To test whether hemichannel-mediated ATP release could directly affect this active cochlear mechanics, we examined the effect of ATP on OHC electromotility. Fig. 2 shows that nanomolar extracellular ATP elicited an inward current in the OHC (Fig. 2*b*) and also altered OHC electromotility (Fig. 2 *c–f*). In Fig. 2*c*, the application of 3.6 nM ATP altered the OHC electromotility-associated nonlinear capacitance. ATP shifted the curve of the nonlinear capacitance to the right (depolarizing) direction. The average shift in peak voltage (V_{pk}) of the nonlinear capacitance was 7.2 ± 0.96 mV ($n = 6$) at 3.6 nM ATP. ATP also reduced electromotility voltage dependence. The slope factor (z) of the voltage dependence was reduced from 0.79 ± 0.03 to 0.69 ± 0.03 ($n = 6$) by application of 3.6 nM ATP. These changes were statistically significant ($P < 0.001$, paired *t* test). The nonlinear capacitance was also reduced by 1.19 ± 0.62 pF ($n = 6$) and showed significant reduction at high concentrations of ATP (Fig. 3*c*). The average reduction in nonlinear capacitance was 3.53 ± 0.57 pF ($n = 9$) at 36 μM ATP ($P < 0.001$, paired *t* test). The ATP effects were reversible and reproducible (Figs. 2*d* and 3 *b* and *c*). ATP could also reversibly reduce OHC electromotility-generated distortion products (Fig. 2 *e* and *f*). Application of 3.6 nM ATP significantly reduced the $2f_1 - f_2$ distortion product from 9.61 ± 2.37 to -0.50 ± 2.77 dB (re: 0.01 nA, $n = 5$) by 10.1 dB ($P < 0.001$, paired *t* test). However, there was no significant change in fundamental frequencies; the f_1 and f_2 components

were reduced by only 2.19 ± 0.65 dB (from 70.72 ± 0.70 to 68.52 ± 0.81 dB) and 2.29 ± 0.67 dB (from 70.88 ± 0.75 to 68.59 ± 0.88 dB), respectively, at 3.6 nM ATP ($P > 0.1$, paired t test).

Extracellular ATP as a cell-signaling molecule can activate purinergic (P2) receptors on the cell surface to influence many aspects of cellular function. P2 receptor expression has been identified in cochlear cells, including OHCs (25–29). Fig. 3*a* shows that immunofluorescent staining of OHCs for P2x2 receptors was strongly positive on the stereocilia, cuticular plate, and basal end. Immunofluorescent staining also demonstrated strong positive labeling of P2x7 receptors on the OHC basolateral wall (Fig. 3*aIII*). Patch clamp recording shows that blockage of P2 receptors negated the effect of ATP on OHC electromotility (Fig. 3 *b* and *c*). Application of 50 μM pyridoxalphosphate-6-azophenyl-2′,4′-disulfonic acid (PPADS) completely abolished both the ATP-induced shift in V_{pk} and the decrease in nonlinear capacitance. The elimination was reversible as the response to ATP was restored after PPADS washout (Fig. 3 *b* and *c*). However, the PPADS itself (indicated by a central bar in Fig. 3 *b* and *c*) did not affect the nonlinear capacitance. The influence of ATP on OHC electromotility was also inhibited by 0.1 mM suramin (data not shown). The data indicate that the effect of ATP on OHC electromotility is through activation of P2 receptors.

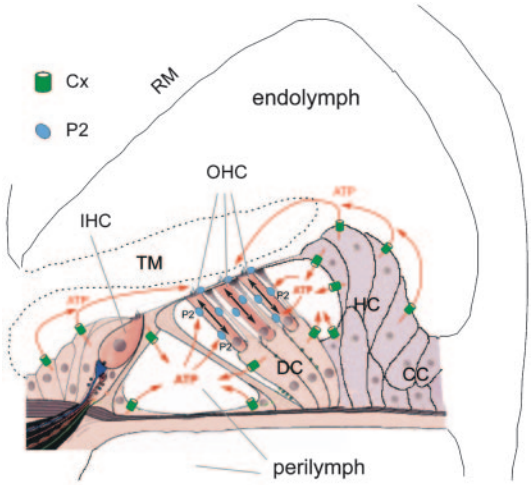

Fig. 4. Schematic drawing of proposed intercellular signaling pathways between supporting cells and OHCs in the cochlea. ATP released from cochlear-supporting cells via connexin hemichannels enters into the EL and PL and consequently acts on the P2 receptors on the OHC's stereocilia and cuticular plate, and lateral wall surface to mediate electromotility. IHC, inner hair cell; DC, Deiters cell; HC, Hensen cell; CC, Claudius cell; TM, tectorial membrane; RM, Reissner's membrane.

Discussion

In a previous study (6), we reported that that connexin hemichannels can activate on the cochlear-supporting cell surface and uptake dyes. In this experiment, we showed that hemichannels on the cochlear-supporting cells could release ATP under physiological conditions; the level corresponded with physiological ATP concentrations in the cochlea (Fig. 1). The data also showed that nanomolar concentrations of extracellular ATP could alter OHC electromotility through activation of P2 purinergic receptors (Figs. 2 and 3). *In vivo*, the apical pole of hair cells extends into the EL, and its lateral wall and basal pole are bathed in the PL. Supporting cells surround hair cells and are also bathed in the PL and EL by separation of the reticular lamina, which is formed by tight junctions at the apical scalar media end of the cells (Fig. 1*a* and 4). There is connexin expression on both apical and basolateral surfaces of the supporting cells (2). Therefore, ATP can be released directly into the PL and EL from the supporting cells through hemichannels and consequently acts on P2 receptors on the OHC surface to alter OHC electromotility (Fig. 4). It has long been known that the cochlear PL and EL contain nanomolar concentrations of ATP that can mediate cochlear and hearing functions (26, 30–32). However, the origin of the intracochlear ATP and the mechanism of its effects remain unclear. Our experiments documented that hemichannels in cochlear-supporting cells could release ATP, which provides a potential source of ATP in the cochlea. The data also revealed that extracellular ATP can directly modify OHC electromotility through activation of P2 receptors, suggesting that there is a hemichannel-mediated intercellular signaling pathway between supporting cells and hair cells to control hearing sensitivity (Fig. 4).

This hemichannel-mediated purinergic intercellular signaling pathway can play an important role in cochlear function. It has been reported that the Ca^{2+} concentration in the EL is very low (only ≈0.02 mM) (33). Cochlear hemichannels can open in such a low Ca^{2+} environment (6) to release ATP (Fig. 1). In the PL, the Ca^{2+} concentration is 0.6–0.7 mM (33), which is considered to be overestimated, and fluctuates decreasing below 0.5 mM. The levels of hemichannel ATP release at 0.5–2 mM extracellular Ca^{2+} were 1.58 ± 0.059 and 0.95 ± 0.054 × 10^{-13} mol, or, 15.8 ± 0.59 and 9.5 ± 0.54 nM, respectively (Fig. 1*d*). There was a 6.3-nM increase in the ATP release when Ca^{2+} decreased from 2 mM to 0.5 mM (Fig. 1*d*). In addition, gap junctional blockers or 5 mM Ca^{2+} could further reduce ATP level below that at 2 mM Ca^{2+} (Fig. 1 *b–d*), implying that a small number of connexin hemichannels remain open even at 2 mM Ca^{2+}. A nanomolar change in ATP level could significantly alter OHC electromotility (Fig. 2). If a small proportion of hemichannels open under normal physiological conditions, they could apparently raise the local ATP level in the vicinity of the hemichannels and, as a consequence, dramatically influence hair cell function (Figs. 3 and 4). It has been reported that ATP could affect sound transduction and neurotransmission (26, 30–32). Intracochlear perfusion of ATP could reduce and inhibit the cochlear microphonics, the compound action potential, and distortion product otoacoustic emissions. Consistent with these reports, we found that ATP could activate P2 receptors to reduce the OHC electromotility and its voltage dependence and to shift its operating point (Fig. 1–3). These effects can reduce the active cochlear mechanics and hearing sensitivity.

Mechanical stimulation also induced hemichannels to release ATP (Fig. 1*c*, and also see refs. 16–18 and 20). Under physiological conditions, cochlear-supporting cells are subjected to mechanical stimulation or membrane tension because of acoustic stimulation-induced basilar membrane vibrations. As sound intensity increases, hemichannel ATP release would increase and in turn reduce OHC electromotility (Fig. 4), which is an active cochlear amplifier to amplify the basilar membrane vibration and enhance hearing sensitivity and frequency selectivity (11, 22–24). Therefore, hemichannel-mediated ATP release in the cochlea may provide a negative feedback between supporting cells and hair cells to control this OHC electromotility-formed active cochlear amplifier. This control is also consistent with the concept that active cochlear mechanics should perform at low intensities to enhance auditory sensitivity (24) and suggests a protective role of this hemichannel-mediated intercellular signaling pathway at high intensities.

This purinergic intercellular signaling pathway can function under physiological conditions. In general, one viable somatic cell contains ≈1 pg (10^{-12} g) or ≈2 fmol (2 × 10^{-15} mol) of ATP. According to the hair cell numbers and the ratio of hair cells and supporting cells in the mammalian cochlea, the total estimated

number of cochlear-supporting cells would be >50,000. The measured amounts of ATP released at 0, 0.5, and 2 mM Ca^{2+} were 4.67, 1.58 and 0.95 $\times$ 10^{-13} mol (Fig. 1). If we assume that every cell is activated, each cell would release 0.467, 0.158, and 0.095% of its cellular ATP, respectively, which occupied only a very small portion of its cellular ATP. If we consider that all cells may not open hemichannels simultaneously and some supporting cells, such as Hensen cells, are not directly exposed to the PL and EL, and assume only 1/10 of supporting cells to be activated, the amount of ATP released per cell would be raised to 4.67, 1.58, and 0.95% at 0, 0.5 and 2 mM Ca^{2+}, respectively. Each cell still released only a small portion of its cellular ATP. As an index of connexin hemichannel leakage, this ATP release also indicates that hemichannels can function in cochlear-supporting cells under normal physiological conditions without an apparent lethal effect.

This experiment showed that connexin hemichannels can release ATP to affect OHC electromotility. The relationship between this release and Cx26 mutation-induced hearing loss is currently unclear. However, ATP as an extracellular signaling modulator can broadly influence cell function. Further studies are required to explore other effects of this hemichannel-mediated ATP release on the cochlear hearing function.

We thank P. G. Wilson for technical support and Drs. Steven R. Post and Reto Asmis for kind help and comments on ATP measurement. This work was supported by National Institute on Deafness and Other Communication Disorders Grants DC 04618 and DC 05989.

1. Kelsell, D. P., Dunlop, J., Stevens, H. P., Lench, N. J., Liang, J. N., Parry, G., Mueller, R. F. & Leigh, I. M. (1997) *Nature* **387,** 80–83.
2. Kikuchi, T., Kimura, R. S., Paul, D. L. & Adams, J. C. (1995). *Anat. Embryol.* **191,** 101–118.
3. Lautermann, J., ten Cate, W. J. F., Altenhoff, P., Grümmer, R., Traub, O., Frank, H. G., Jahnke, K. & Winterhager, E. (1998) *Cell Tissue Res.* **294,** 415–420.
4. Santos-Sacchi, J. & Dallos, P. (1983) *Hear. Res.* **9,** 317–326.
5. Zhao, H. B. & Santos-Sacchi, J. (2000) *J. Membr. Biol.* **175,** 17–24.
6. Zhao, H. B. (2005) *Eur. J. Neurosci.* **21,** 1859–1868.
7. Harris, A. L. (2001) *Q. Rev. Biophys.* **34,** 325–472.
8. Evans, W. H. & Martin, P. E. (2002). *Mol. Membr. Biol.* **19,** 121–136.
9. Bennett, M. V. L., Contreras, J. E., Bukauskas, F. F. & Saez, J. C. (2003). *Trends Neurosci.* **26,** 610–617.
10. Goodenough, D. A. & Paul, D. L. (2003). *Nat. Rev. Mol. Cell Biol.* **4,** 285–294.
11. Zhao, H. B. & Santos-Sachi, J. (1999) *Nature* **399,** 359–362.
12. Santos-Sacchi, J. & Zhao, H. B. (2003). *Pflügers Arch.* **446,** 617–622.
13. Santos-Sacchi, J., Kakehata, S. & Takahashi, S. (1998) *J. Physiol. (London)* **510,** 225–235.
14. Thorne, M., Salt, A. N., DeMott, J. E., Henson, M. M., Henson, O. W., Jr., & Gewalt, S. L. (1999). *Laryngoscope* **109,** 1661–1668.
15. Munoz, D. J., Thorne, P. R., Housley, G. D. & Billett, T. E. (1995) *Hear Res.* **90,** 119–125.
16. Romanello, M., Pani, B., Bicego, M. & D'Andrea, P. (2001). *Biochem. Biophys. Res. Commun.* **289,** 1275–1281.
17. Stout, C. E., Costantin, J. L., Naus, C. C. & Charles, A. C. (2002). *J. Biol. Chem.* **277,** 10482–10488.
18. Leybaert, L., Braet, K., Vandamme, W., Cabooter, L., Martin, P. E. & Evans, W. H. (2003). *Cell Commun. Adhes.* **10,** 251–257.
19. Bao, L., Sachs, F. & Dahl, G. (2004) *Am. J. Physiol. Cell Physiol.* **287,** C1389–C1395.
20. Gomes, P., Srinivas, S. P., Van Driessche, W., Vereecke, J. & Himpens, B. (2005) *Invest. Ophthalmol. Vis. Sci.* **46,** 1208–1218.
21. Zhao, H. B. & Santos-Sacchi, J. (1998) *J. Gen. Physiol.* **112,** 447–455.
22. Brownell, W. E., Bader, C. R., Bertrand, D. & Ribaupierre, Y. (1985) *Science* **227,** 194–196.
23. Ashmore, J. F. (1987) *J. Physiol. (London)* **388,** 323–347.
24. Dallos, P. (1992) *J. Neurosci.* **12,** 4575–4585.
25. Housley, G. D., Greenwood, D. & Ashmore, J. F. (1992). *Proc. Biol. Sci.* **249,** 265–273.
26. Housley, G. D., Kanjhan, R., Raybould, N. P., Greenwood, D., Salih, S. G., Jarlebark, L., Burton, L. D., Setz, V. C., Cannell, M. B. & Soeller, C. (1999) *J. Neurosci.* **19,** 8377–8388.
27. Brandle, U., Zenner, H. P. & Ruppersberg, J. P. (1999) *Neurosci. Lett.* **273,** 105–108.
28. Chen, C. & Bobbin, R. P. (1998) *Br. J. Pharmacol.* **124,** 337–344.
29. Parker, M. S., Onyenekwu, N. N. & Bobbin, R. P. (2003) *J. Am. Acad. Audiol.* **14,** 286–295.
30. Bobbin, R. P. & Thompson, M. H. (1978). *Ann. Otol. Rhinol. Laryngol.* **87,** 185–190.
31. Kujawa, S. G., Erostegui, C., Fallon, M., Crist, J. & Bobbin, R. P. (1994) *Hear. Res.* **76,** 87–100.
32. Munoz, D. J., Thorne, P. R., Housley, G. D., Billett, T. E. & Battersby, J. M. (1995) *Hear. Res.* **90,** 106–118.
33. Slat, A. N. & Thalmann, R. (1988) in *Physiology of the Ear*, eds. Jahn, A. F. & Santos-Sacchi, J. (Raven, New York), pp. 341–357.